Applied Surface Science 396 (2017) 1435–1442

Contents lists available at ScienceDirect

Applied Surface Science

journal homepage: www.elsevier.com/locate/apsusc

Full Length Article

Dense and high-stability Ti_2AlN MAX phase coatings prepared by the combined cathodic arc/sputter technique

Zhenyu Wang[a,b], Jingzhou Liu[a], Li Wang[a], Xiaowei Li[a], Peiling Ke[a,*], Aiying Wang[a,*]

[a] Key Laboratory of Marine Materials and Related Technologies, Zhejiang Key Laboratory of Marine Materials and Protective Technologies, Ningbo Institute of Materials Technology and Engineering, Chinese Academy of Sciences, Ningbo 315201, China
[b] University of Chinese Academy of Sciences, Beijing 100049, China

ARTICLE INFO

Article history:
Received 7 September 2016
Received in revised form
10 November 2016
Accepted 23 November 2016
Available online 24 November 2016

Keywords:
Nano-laminate
MAX phases
Combined cathodic arc/sputter
Dense
High-stability

ABSTRACT

Ti_2AlN belongs to a family of ternary nano-laminate alloys known as the MAX phases, which exhibit a unique combination of metallic and ceramic properties. In the present work, the dense and high-stability Ti_2AlN coating has been successfully prepared through the combined cathodic arc/sputter deposition, followed by heat post-treatment. It was found that the as-deposited Ti-Al-N coating behaved a multilayer structure, where (Ti, N)-rich layer and Al-rich layer grew alternately, with a mixed phase constitution of TiN and $TiAl_x$. After annealing at 800 °C under vacuum condition for 1.5 h, although the multilayer structure still was found, part of multilayer interfaces became indistinct and disappeared. In particular, the thickness of the Al-rich layer decreased in contrast to that of as-deposited coating due to the inner diffusion of the Al element. Moreover, the Ti_2AlN MAX phase emerged as the major phase in the annealed coatings and its formation mechanism was also discussed in this study. The vacuum thermal analysis indicated that the formed Ti_2AlN MAX phase exhibited a high-stability, which was mainly benefited from the large thickness and the dense structure. This advanced technique based on the combined cathodic arc/sputter method could be extended to deposit other MAX phase coatings with tailored high performance like good thermal stability, high corrosion and oxidation resistance etc. for the next protective coating materials.

1. Introduction

Ternary layered nitrides Ti_2AlN (space group $P6_3/mmc$) belongs to a family of the so-called $M_{n+1}AX_n$ phases, where M is a transition metal, A is an A group element, X is either C or N, and n = 1–3. MAX phases are well known for their unique structure and interesting properties combining those of ceramics and metals, such as high electrical and thermal conductivity, good machinability, excellent thermal shock resistance, as well as superior oxidation and corrosion resistances etc. [1,2]. So far, Ti_2AlN MAX phases have been synthesized in both bulk and coating form by various methods. In particular, surface coating approach can take full advantage of superior properties of both MAX phases and substrate materials, which thereafter improve the structural and physi-chemical stabilities of the substrate materials under harsh conditions, such as high temperature, high corrosion as well as high irradiation in fields of aerospace, nuclear systems [3,4].

In terms of the preparation for Ti_2AlN coatings, many studies focused on the epitaxial growth of single crystalline Ti_2AlN coating on heated single-crystalline MgO or Al_2O_3 substrates by reactive magnetron sputtering, where the Ti, Al or TiAl targets in a mixed Ar-N_2 source gases were used [5–8]. Very recently, two-step method was also attempted to synthesize Ti_2AlN MAX phase coating, in which the Ti-Al-N coating with appropriate composition was firstly deposited using reactive magnetron sputtering, followed by heat treatment in vacuum [9,10]. Moreover, investigations on the phase stability and oxidation behavior of the Ti_2AlN coating have been conducted [5,11,12]. It was found that the Ti_2AlN coating suffered serious degradation from the vacuum treatment or oxidation process, due to its loose and columnar structure with limited coating thickness by traditional sputtering methods. Considering the perspective applications, it is prerequisite to fabricate the denser, higher-stability and thicker Ti_2AlN coatings by developing an advanced synthesis technique.

Among the physical vapor deposition (PVD) methods, vacuum cathodic arc deposition (VAD) technique has drawn much attention for the deposition of nitride and carbide coatings, due to its high ionization degree, high deposition rate, strong coating/substrate

* Corresponding authors.
E-mail addresses: kepl@nimte.ac.cn (P. Ke), aywang@nimte.ac.cn (A. Wang).

http://dx.doi.org/10.1016/j.apsusc.2016.11.183
0169-4332/

adhesion etc. [13,14]. Now as one of the perspective PVD techniques, VAD coatings have been widely used in cutting tools, molds and mechanical components, i.e., to improve their mechanical, wear-resistant or oxidation-resistant properties as well as lifetime [15,16]. Recently, various VAD methods have been successfully utilized to prepare Ti_2AlC, Ti_2AlN and Cr_2AlC coatings. Rosén and Guenette et al. [17,18] have directly synthesized epitaxial and highly orientated Ti_2AlC film on a-Al_2O_3 (001) single crystal substrate, using a pulsed VAD method with elemental Ti, Al, and C cathodes at 900 °C. In addition, Cr_2AlC coating has been achieved through VAD method from Cr_2AlC target combined with heat post-treatment [19]. Previous works have proved that the preparation of MAX phase coatings using VAD method is available, but there are many defects needed to be overcome such as macro-particles and holes in these coatings due to the low melt point of the Al-containing compound target. Increasing the partial pressure of reactive gas or modifying the magnetic filtering during the reactive VAD process can reduce the above mentioned defects to some extent [20], but it is known empirically that low reactive gas partial pressure is essential to form the MAX phase coating with dense structure [21].

In the present work, we deposited the Ti_2AlN coating by a combined cathodic arc/sputter technique and subsequent vacuum heat treatment, in order to dense structure, increase deposition rate, and low deposition temperature as well. In addition, Ti-6Al-4V was selected as the substrates, because titanium alloys were used widely ranging from aerospace and marine to biomedical areas due to its high specific strength, chemical stability and good biocompatibility [22]. During coating deposition, Ti element was provided by VAD Ti target way while Al was introduced by sputtering source. The phase formation and microstructure evolution of the as-deposited Ti-Al-N coating after heat treatment were investigated using XRD, SEM and TEM. Furthermore, the vacuum thermal behavior of the obtained Ti_2AlN MAX phase coating was addressed in terms of the structural evolution.

2. Experimental methods

The samples of Ti-6Al-4V (TC4) with the size of 15 mm × 10 mm × 2 mm were used as the substrates. The nominal composition of this alloy in weight per cent is: Al, 6.04; V, 4.03; Fe, 0.3; O, 0.1; C, 0.1; N, 0.05; H, 0.015 and the balance Ti. After being polished to 3000-grit, the substrates were ultrasonically cleaned in acetone and ethanol each for 15 min followed by a dried process in warm air. Ti-Al-N coatings were deposited by a combined cathodic arc/sputter system. Fig. 1 shows the schematic feature of the hybrid system used in this experiment. The circular titanium target (purity of 99.9%) was used as an arc cathode source, and the rectangular aluminum target (purity of 99.9%) was used for the sputtering source. Gas mixtures of Ar (99.999%) and N_2 (99.999%) at a mixing ratio of N_2:Ar = 1:10 were used as reactive gas sources. The substrates were fixed on a rotary sample holder at the front of Al target with a distance of 5 cm to the target. Prior to deposition, the TiN diffusion barrier about 600 nm were fabricated to avoid inter diffusion of elements between coating and substrates in the later thermal treatment process. During deposition, the arc power to the Ti target and the sputter power to the Al target were controlled at 18 W and 3.1 kW, respectively. The working pressure was kept at about 2.0 Pa by controlling the valve of the vacuum chamber. The DC negative bias voltage of −200 V was applied to the substrates without other intentional heating. The detailed conditions of the coating process are listed in Table 1. After 90 min deposition, the thickness of the coating was about 7.12 μm. Then, annealing treatment of the as-deposited Ti-Al-N coating was conducted at 800 °C in vacuum for 1.5 h. Before the annealing process, the tube

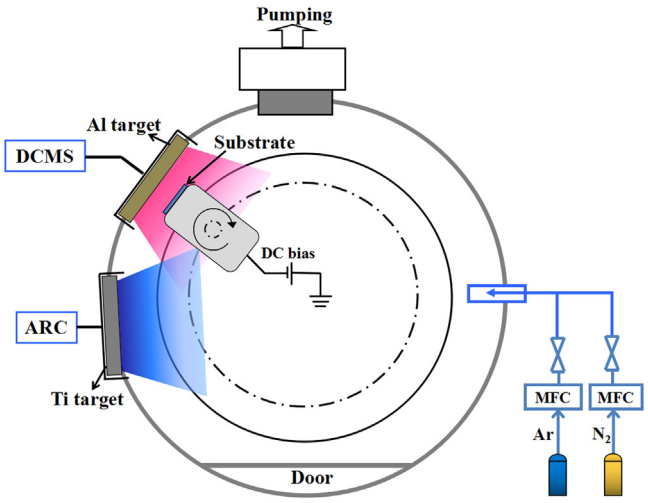

Fig. 1. Schematic diagrams of the combined cathodic arc/sputter technique.

Table 1
Deposition conditions for Ti-Al-N coatings by the combined cathodic arc/sputter technique.

	TiN diffusion barrier	Ti-Al-N coating
Ti target power (Arc)	18 W	18 W
Al target power (Sputter)	0 kW	3.1 kW
Total pressure	8 Pa	2 Pa
Ar/N_2 flow rate	0 sccm/600 sccm	20 sccm/200 sccm
Deposition temperature	200 °C	200 °C
Substrate bias voltage	−100 V	− 200 V
Substrate holder rotation	5 rpm	5 rpm
Deposition time	5 min	90 min

furnace was pump down to 1.0×10^{-2} Pa and heated to the annealing temperature with a heating rate of about 4 K/min.

The microstructures of the coating were investigated by the combined scanning electron microscopy (SEM), and transmission electron microscopy (TEM). Structural analysis was carried out using X-ray diffraction (XRD), with a BrukerD8 Advance diffractometer, using Cu Kα radiation. Raman spectroscopy (InVia-reflex, Renishaw) equipped with a 60 mW He–Ne laser of 532 nm exciting wavelength was used to evaluate the MAX phase structure. The surface secondary electrons morphology and cross-section backscattered electrons morphology were examined by a FEI Quanta FEG 250 SEM, equipped with an energy-dispersive X-ray spectrometry (EDX) using an EDAX Sapphire Si (Li) detector. Chemical composition was measured by the EDX. Cross-sectional TEM specimens were prepared with a focused ion beam (FIB) equipment (Auriga, Zeiss). Details of cross sectional TEM sample preparation using FIB are given in Ref. [23]. Cross-sectional TEM (XTEM) studies were performed on a TF-20 system. The coating stability was evaluated by high-vacuum (~7.0×10^{-3} Pa) annealing at 900 and 1000 °C. At each temperature, the sample was held constant for 1 h, followed by the phase structure measurement.

3. Results and discussion

3.1. Phase structure and composition

Fig. 2 shows the XRD patterns of the as-deposited Ti-Al-N coating and the annealed one for comparison. The as-deposited coating was mainly composed of FCC-TiN (PDF#38-1420) and $TiAl_x$ intermetallic phases. But the diffraction peaks of $TiAl_x$ intermetallic phases were located between peaks of Ti (PDF#65-3362) and $Ti_{19}Al_6$ (PDF#65-8567), suggesting x varies from 0 to 6/19.

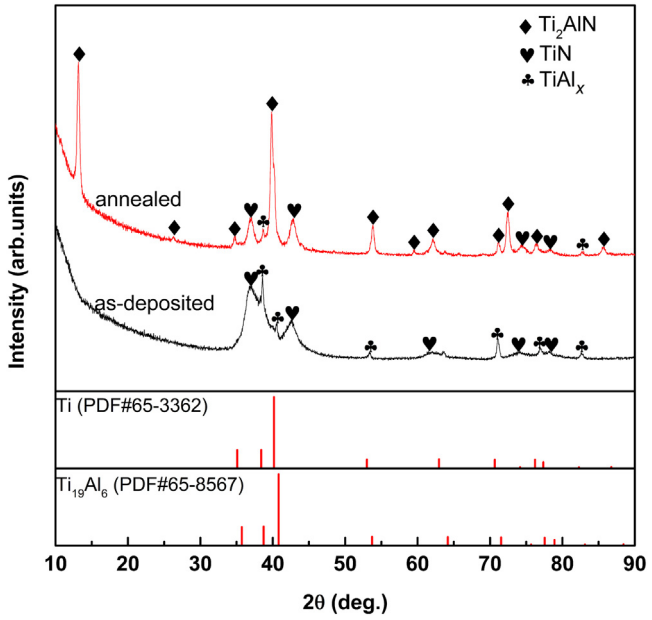

Fig. 2. XRD patterns of the as-deposited Ti-Al-N coating and the annealed one.

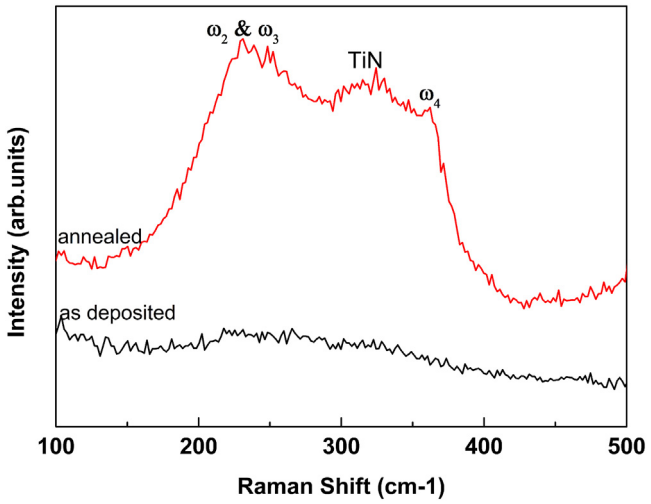

Fig. 3. Raman spectra of the as-deposited Ti-Al-N coating and the annealed one.

Table 2
Chemical composition and thickness of the as-deposited and annealed coating.

Sample	Chemical composition		Thickness (μm)
	Ti	Al	
as-deposited coating	63.68 ± 0.28	20.35 ± 0.10	7.12 ± 0.24
annealed coating	63.87 ± 0.53	20.39 ± 0.49	7.09 ± 0.18

Furthermore, the TiN diffraction peak at about 36.7° and 42.6° exhibited a broad feature, which was indicative of weak degree of crystallinity or very fine grains. Similar results were found in Ref. [24], where the Ti-Al-N coatings were deposited by magnetron sputtering Ti_2AlN target without intentional substrate heating. However, amorphous Cr-Al-C coating was obtained by Li et al. [19], using the VAD method from Cr_2AlC target in the unintentional heating condition. Since high temperature generally plays a key factor to synthesize MAX phase coating [2], it is expected that no crystalline Ti_2AlN MAX phase existed in the as-deposited coating, probably due to the relatively low deposition temperature used in this study.

In order to promote the formation of Ti_2AlN MAX phase, the heat post-treatment for the as-deposited Ti-Al-N coating was conducted under a high vacuum condition. After annealing at 800 °C for 1.5 h, quantitative analysis reveals that the crystalline phases presenting in the annealed coating are the dominant Ti_2AlN phase (81.7 wt.%) with 16.2 wt.% TiN and 2.1 wt.% $TiAl_x$. In addition, the peaks of TiN and $TiAl_x$ phases became sharper and weaker as compared to that of the as-deposited one. As a consequence, it could be deduced that the formation of Ti_2AlN MAX phase was due to the solid reactions among TiN, $TiAl_x$, and other undetected Al-rich phases [11]. However, it is worth noting that the solid reaction temperature presented in this study is lower about 500 °C than the formation temperature in bulk Ti_2AlN. Taking priority of this advanced technique, the homogeneous mixture of the Ti, Al and N elements at atomic level results in the shorter diffusion distance during reaction process [25,26], which is the key reason to understand the obtained lower temperature to form the Ti_2AlN MAX phase in this case.

Raman spectroscopy is a powerful technique for characterizing Ti_2AlN MAX phase compounds, as there are four Raman active modes ($2E_{2g}$, E_{1g} and A_{1g} at 147 cm^{-1}, 228 cm^{-1},224 cm^{-1} and 360 cm^{-1}; named ω_1, ω_2, ω_3 and ω_4, respectively) in the 211 phases [27]. As shown in Fig. 3, Peaks at 224, 228 and 360 cm^{-1}, absent from the as-deposited one, are displayed in the spectrum of annealed Ti-Al-N coating, which correspond well to the ω_2–ω_4 modes of reported Ti_2AlN phase, despite that the additional peak at 320 cm^{-1} in the spectrum related to the acoustic phonon modes of TiN phase [28]. Combined with the XRD analysis, it could be confirmed that the Ti_2AlN MAX phase formed successfully in the annealed Ti-Al-N coating. However, noted that the mode associated with ω_1 was not observed in the measured spectrum.

Table 2 illustrated the chemical composition of the as-deposited Ti-Al-N coating and annealed one using EDX analysis. N content was not shown here because of the possible deviation of light element by EDX technique, but it has a significant effect on the Ti_2AlN formation mechanisms [29], which will be considered in our next research. It is interesting that the annealed Ti-Al-N coating owned the similar atomic ratio of Ti:Al = 3.13 and thickness to that of the as-deposited one. Comparing with the high-pure Ti_2AlN phase acquired by annealing treatment with the atomic ratio of Ti:Al = 2:1 [30], the Al content is insufficient in this study, which leads to the residual TiN phase in the annealed coating. Therefore, supplying more Al content in the coating will be a guide concept to obtain the high purity of Ti_2AlN phase in the future works.

3.2. Morphology and microstructure

Fig. 4 shows the SEM surface images of the as-deposited and annealed Ti-Al-N coating. Both the as-deposited and annealed coatings exhibited compact and crack-free microstructure, except some macro-particles displayed in the coating surface, which is a typical feature of unfiltered cathodic arc deposition [31]. In addition, both the cross-sectional morphologies of the as-deposited Ti-Al-N coating and annealed one exhibited the dense, homogenous structures with no visible voids across the coating depth and the strong adhesion to the TC4 substrate as well. As for the as-deposited coating, there were a ~0.8 μm thick inner TiN adhesive layer and a ~7.1 μm thick outer Ti-Al-N layer.

To further identify the composition of macro-particles and smooth coating area, Fig. 5 illustrates the backscattered SEM surface image and the corresponding element mapping for annealed Ti-Al-N coating. Obviously, the macro-particles demonstrated different contrast to the smooth area, suggesting the various chemical compositions in these regions, as shown in Fig. 5a. The Ti and Al element mapping, shown in Fig5.b and c, displayed that the macro-particles were enriched in Ti and poor in Al. This indicated that these

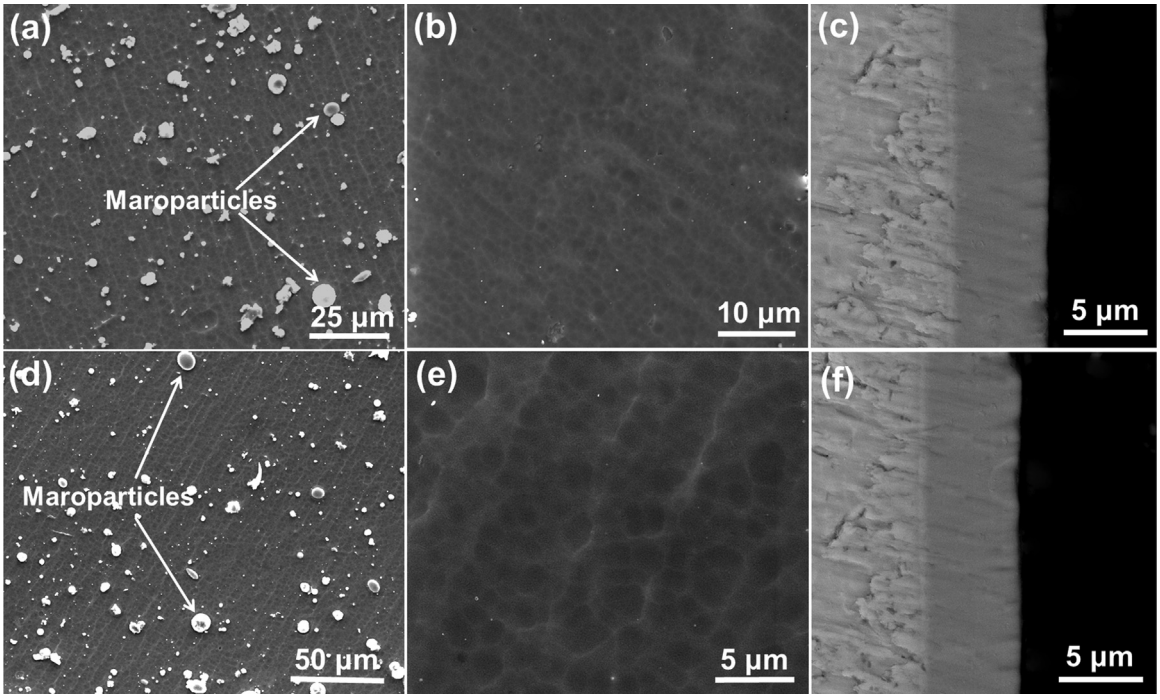

Fig. 4. Surface and cross-sectional morphologies of (a), (b), (c) the as-deposited Ti-Al-N coating and (d), (e), (f) the annealed one.

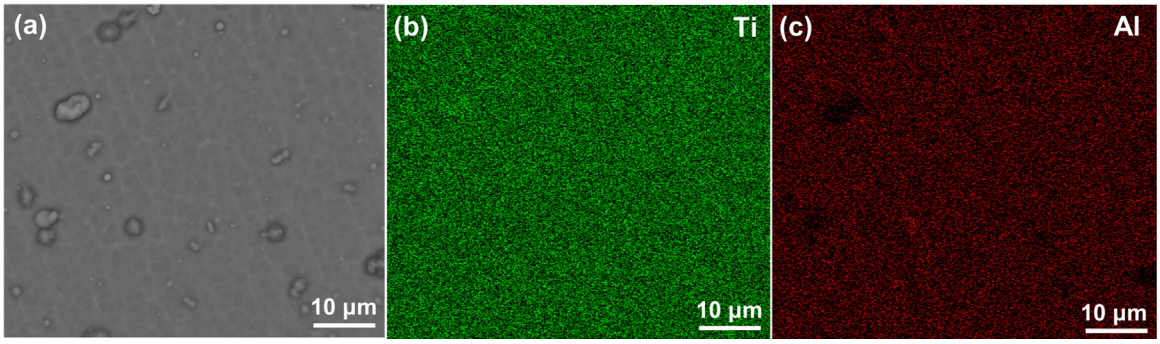

Fig. 5. Surface backscattered morphologies of the annealed Ti-Al-N coating (a) and (b) Ti, (c) Al element mapping.

macro-particles were mainly ascribed to the ejected liquid droplets from the Ti target during arc discharge. However, compared with other work [19], where the MAX phase coating was prepared only by cathodic arc deposition, the important result here is that the numbers of the macro-particles were greatly reduced due to the benefits from the combined cathodic arc/sputter technique.

The microstructure of the as-deposited and annealed Ti-Al-N coatings was further studied by TEM and HRTEM. Fig. 6a shows a typical cross-sectional TEM bright-field image and corresponding selected area electron diffraction (SAED) pattern of the as-deposited coatings. The inner TiN layer and outer Ti-Al-N layer could be clearly distinguished from the TEM image, and the TiN layer displayed the characteristics of a columnar structure. However, the outer Ti-Al-N layer (shown in Fig. 6b) evolved in the multilayer structure, in which the bright and dark layer originated from their different electron scattering factor alternately was visible along the direction perpendicular to the surface. Moreover, the bilayer period of the as-deposited coating was about 15 nm, consisting of ~10 nm dark layer and ~5 nm bright layer, as illustrate in Fig. 6c. In the HRTEM image (Fig. 6d), one observed lattice fringes, corresponding to TiN and $TiAl_x$, mainly inside the dark layer, the bright layer looking rather structureless. Further STEM image shown in Fig. 7a indicated that the multilayer structure with alternating dark and bright contrast layer was clearly identified. Noted that, the STEM technique reveals atomic number (Z) contrast [32], thus the STEM image reveals opposite contrast of different layers in comparison with that of TEM bright-field image. By recording the EDX line profile along the white line in Fig. 7a, we could distinguish the layers composition composed of Ti, N and Al. Fig. 7b shows the EDX result, where the Al has positive deviation corresponding to the dark layer in the STEM image, while the bright layer has higher Ti and N content. Therefore, combining the TEM and XRD results, we can confirm that the Al-rich layers are mostly amorphous with small and sparse crystals. The appearance of the multi-layer structure in the as-deposited coating prepared by the combined cathodic arc/sputter system is considered to be the effect of sample rotation during deposition, which leads the substrates to periodically face the different target.

For comparison, Fig. 8 shows the TEM results of the annealed Ti-Al-N coating. Similar to that of as-deposited coating, the annealed Ti-Al-N coating remained the dense and crack-free structure, and the multilayer structure still existed after the heat treatment process, as displayed in Fig. 8a and b. However, part of interface became indistinct or disappeared in the coating. Fig. 8c is a high-resolution

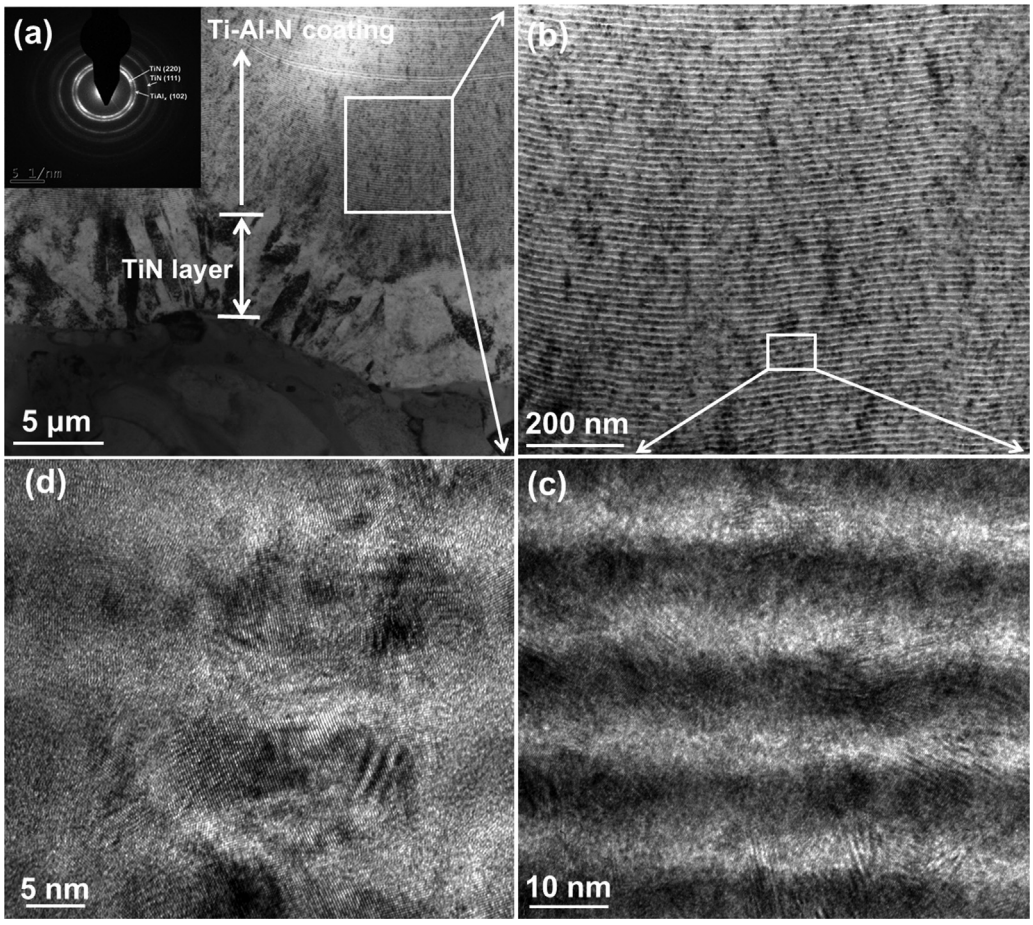

Fig. 6. TEM cross-sectional images of the as-deposited Ti-Al-N coating, (a) Bright-field image with the corresponding SAED pattern, (b)(c) enlarged view of the Ti-Al-N coating and (d) HRTEM image.

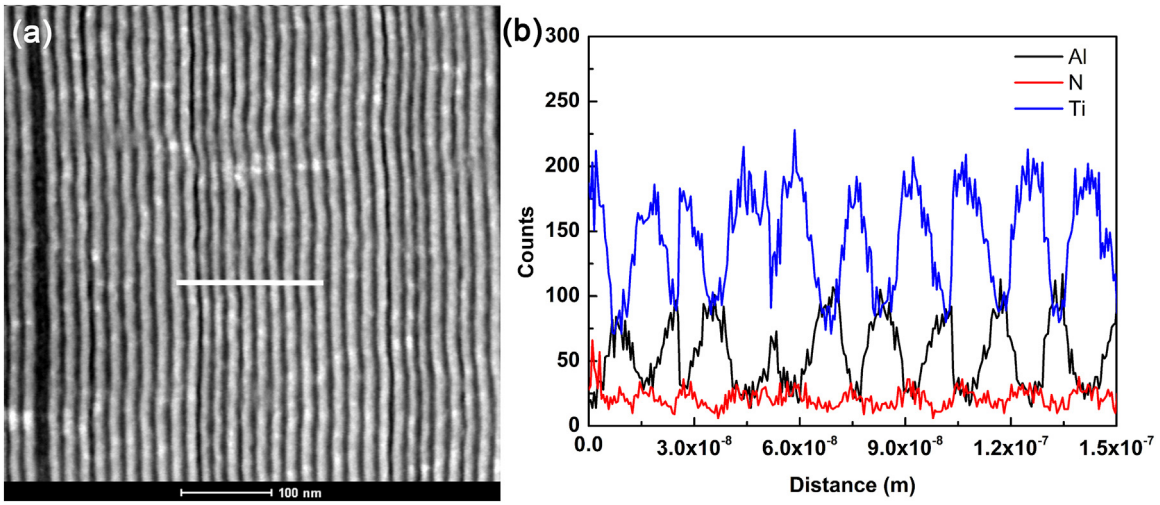

Fig. 7. (a) STEM image of the as-deposited coating and (b) corresponding EDS line-scanning of the white line marked in (a).

image of the annealed coating. A typical micrograph as well as the Fast Fourier Transform (FFT) corresponding to the zone indicated by the square in inset is shown in Fig. 8d. One can clearly identify on this FFT the (000*l*) typical spots of the MAX phase. The stacking sequence orthogonal to the basal plane direction can be seen in the high resolution TEM image (Fig. 8d), with the electron beam paralleling to the [11–20] direction [33]. The c lattice parameter deduced from this high resolution TEM image is 1.36 nm, a value in good agreement with previous measurements [34]. By characterizing the STEM and EDX line profile along the white line in Fig. 9a, it could be seen that, in contrast to that of the as-deposited coating, the thickness ratio of the dark layer to the bright layer increased after the heat treatment. Furthermore, the anti-correlation phenomenon among the content of Ti, N and Al, shown in Fig. 9b, demonstrated the distinct multilayer, where the intensity ratio of the element Al to Ti decreased due to the inter-diffusion of the Al, Ti and N element.

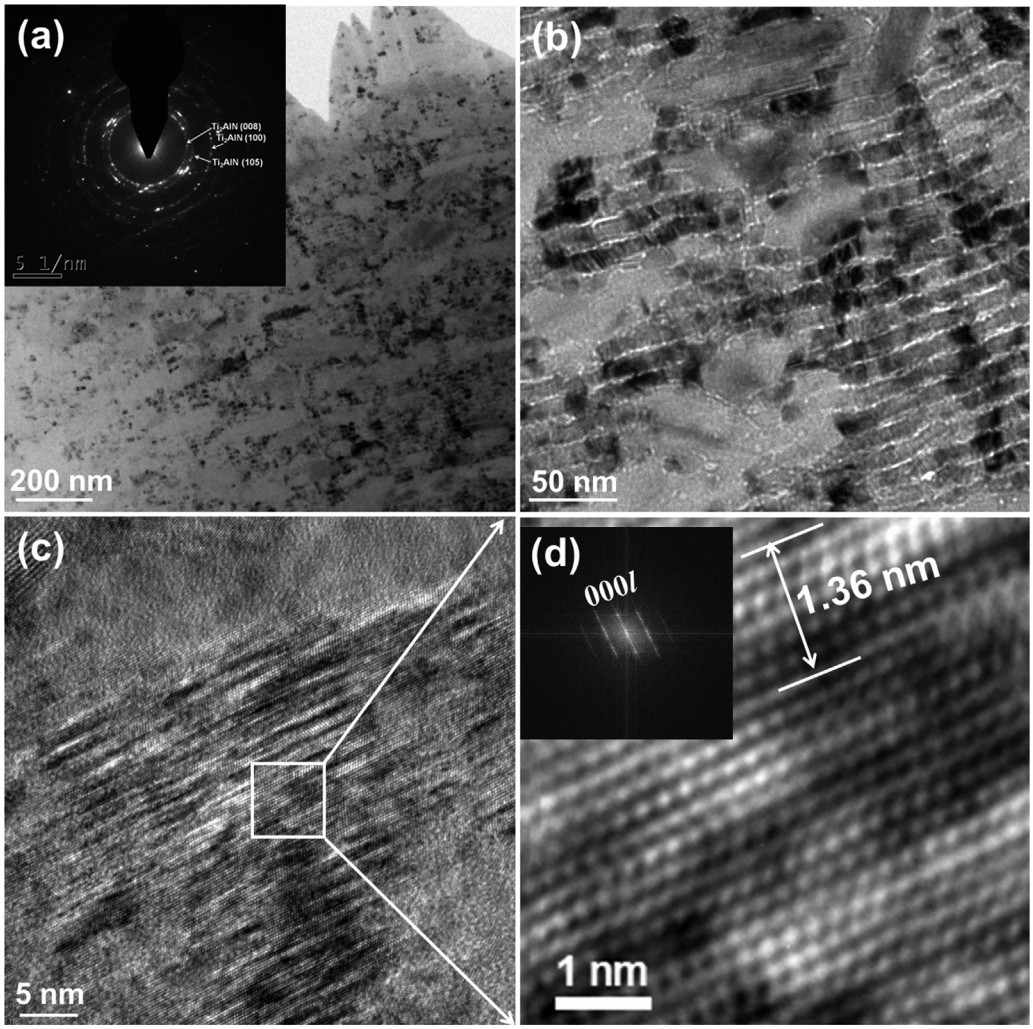

Fig. 8. TEM cross-sectional images of the annealed Ti-Al-N coating, (a) Bright-field image with the corresponding SAED pattern, (b) enlarged view of the Ti-Al-N coating, (c) HRTEM image, (d) enlarged view from the marked area in (c) and corresponding FFT image after periodic filtering processing in (c).

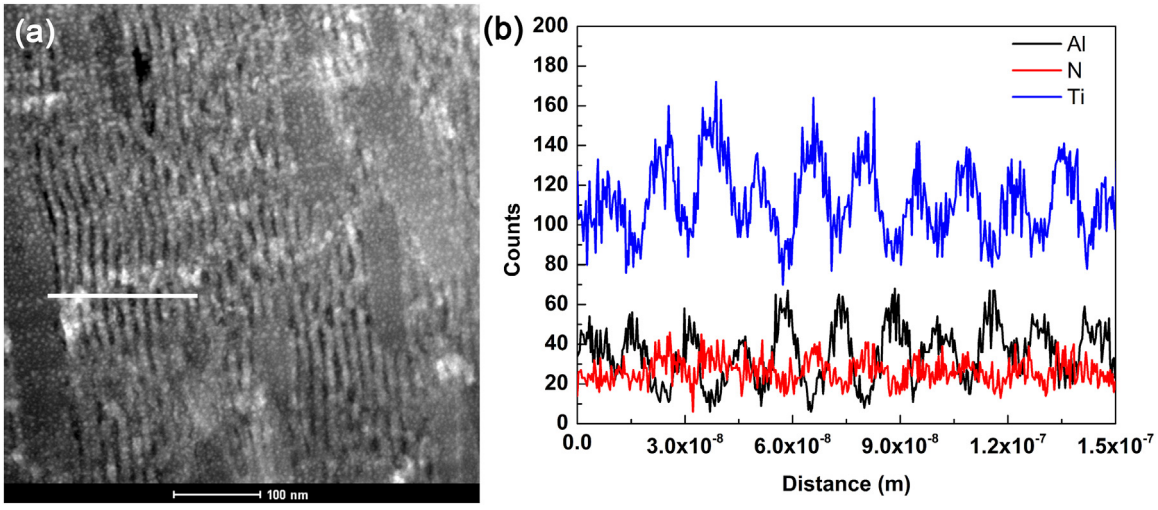

Fig. 9. (a) STEM image of the annealed coating and (b) corresponding EDS line-scanning of the white line marked in (a).

From the above mentioned results, it indicates that the Ti_2AlN phase formation mechanism during annealing originates from the diffusion control of reaction processes contributed to the formation of Ti_2AlN phase: It has been reported that stoichiometric or over-stoichiometric TiN coating annealed in vacuum retained its phase structure and Ti—N bonding cannot be decomposed at 800 °C [35]. The diffusion of Al into TiN phase results in the transformation of the cubic TiN into a (Ti, Al)N cubic solid solution, not the Ti_2AlN

MAX phase. According to the XRD patterns (Fig. 2), the Ti-rich layer mainly composed of TiN and $TiAl_x$, $TiAl_x$ can be fully recognized as a hexagonal structure similar to that of α-Ti metal, but with smaller lattice parameters (higher diffraction angle). It is likely that Al is substitionally dissolved on Ti atomic positions of the hexagonal structure of α-Ti. Indeed, the solubility of light elements such as N is very high in α-Ti and α-Ti_3Al so that they precipitate as Ti_2AlN phases [36]. Therefore, a hexagonal solid solution with α-Ti structure will be transformed to a more ordered structure (Ti_2AlN). This transformation can easily occur due to the very short diffusion distance in the presence of aluminum and nitrogen, a majority of the atomic planes of Ti remaining unchanged. Similar reactive processes have been reported by Cabioch et al. [37] and Grieseler et al. [38], where Ti_2AlN phase was formed at lower temperature about 500–600 °C. Correspondingly, the solid reaction in this case can be described by the following formula:

$$2TiAl_x + Al_{1-2x} + N = Ti_2AlN \quad (1)$$

While, Dolique et al. [36] reported that TiN/TiAl multilayers grown at room temperature by using an ion beam sputtering technique could be transformed upon annealing at 600 °C into (Ti,Al)N/Ti_2AlN multilayers. The reason for the formation of Ti_2AlN phase was that the TiN layers contained nitrogen vacancies (about 20%), which evoked a thermally activated diffusion mechanism involving Ti, Al, and N vacancies that allows a diffusion of Ti atoms from TiN into TiAl layer. In this work, the existence of $TiAl_x$ in the Ti-rich layer indicated that N may be insufficient to form the stoichiometric TiN. Besides, TiN diffraction peaks are quite broad, suggesting the quite small grain sizes or the weak crystallinity. Therefore, it can be concluded that a diffusion of Ti and N atoms from (Ti, N)-rich layer to the Al-rich layer can occur during vacuum treatment, and then Ti_2AlN MAX phase is formed. This solid reaction is more complicated than the above one because of longer diffusion distance. The phase transformation involves a balanced equation as following:

$$2Ti + Al + N = Ti_2AlN \quad (2)$$

3.3. Thermal stability

Thermal stability of the Ti_2AlN phase is crucial for high temperature applications, specially, such as components serving for harsh aerospace engine and nuclear reactive system. MAX phases are known to easily decompose at lower temperatures when they are exposed to vacuum environment, due to the absence of surface oxides as protective diffusion barrier. To determine the phase stability of the formed Ti_2AlN MAX phase coating, we carried out one hour annealing under high vacuum condition with 900 °C and 1000 °C, respectively. As shown in Fig. 10, the diffraction intensity of TiN phase increased and the TiN phase content increased to about 25.5 wt%. Instead, the Ti_2AlN phase content decreased to 70.27 wt.% after 1 h annealing at 900 °C, suggesting that Ti_2AlN phase was decomposed into TiN phase. Moreover, TiN phase content further increased to 39.1 wt.% at 1000 °C and Ti_2AlN phase decreased to 53.78 wt%. Beckers et al. [39] reported that the epitaxially grown Ti_2AlN thin films started to decompose at around 750 °C, while 1 h annealing at 800 °C resulted in an almost complete decomposition of Ti_2AlN. Zhang et al. [12] studied the phase transformation of Ti_2AlN MAX thin film upon annealing in Ultra-High-Vacuum, it was found that Al desorption occurs due to its high vapor pressure when temperature is >600 °C and Ti_2AlN phase is nearly undetected at 900 °C. Although one hour annealing was conducted at 1000 °C in our study, Ti_2AlN phase is still the main phase, indicating that the obtained Ti_2AlN coating exhibited a high-stability. One reason for this is the higher Al content resulting from its much bigger thickness. Another factor is related to its dense structure without obvious defects, such as columnar grain boundaries, micro-crack and voids, which are the fast diffusion channel of the Al to the surfaces under high vacuum condition.

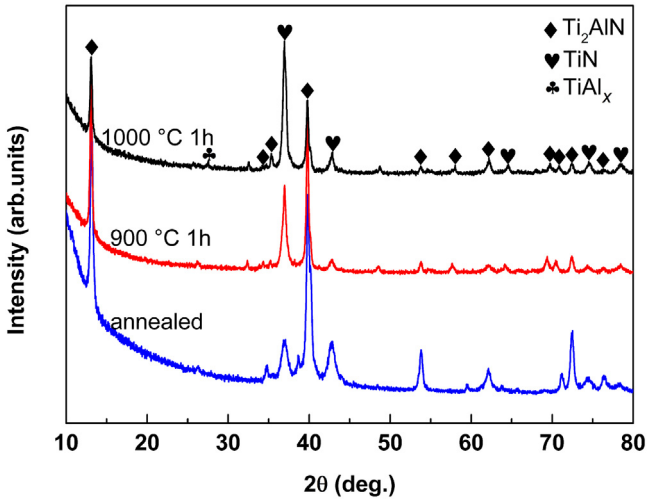

Fig. 10. XRD patterns of the annealed Ti-Al-N coating and the vacuum heat treated coating at 900 °C and 1000 °C.

4. Conclusions

In the present work, the combined cathodic arc/sputter technique was used to prepare the Ti_2AlN MAX phase coating. The main conclusions are drawn as followings:

(1) The as-deposited Ti-Al-N coating exhibited a multilayer structure, containing (Ti, N)-rich layer and Al-rich layer with TiN and $TiAl_x$ ($0 < x < 6/19$) mix phase, from VAD Ti target and sputtering Al target without other intentional heating.
(2) After annealing treatment at 800 °C for 1.5 h under vacuum condition, the solid reaction occurred and Ti_2AlN MAX phase formed as the major phase together with TiN and little $TiAl_x$.
(3) It is suggested that the formed Ti_2AlN MAX phase still remained the major phase after one hour vacuum annealing at 1000 °C, indicating a high-stability. The dense structure and high-stability made obtained Ti_2AlN coating as good candidates for irradiation-/oxidation-/corrosion-resistant applications, such as the protective coatings for nuclear power plants and aerospace components.

Acknowledgments

The research was supported by the National Natural Science Foundation of China (51522106), the National Science and Technology Major Project of China (2015ZX06004-001), and Ningbo Municipal Natural Science Foundation (2015A610073).

References

[1] M. Barsoum, The $M_{N+1}AX_N$ phases: a new class of solids: thermodynamically stable nanolaminates, Prog. Solid State Chem. 28 (2000) 201–281.
[2] P. Eklund, M. Beckers, U. Jansson, H. Högberg, L. Hultman, The $M_{n+1}AX_n$ phases: materials science and thin-film processing, Thin Solid Films 518 (2010) 1851–1878.
[3] Z.J. Feng, P.L. Ke, A.Y. Wang, Preparation of Ti_2AlC MAX phase coating by DC magnetron sputtering deposition and vacuum heat treament, J. Mater. Sci. Technol. 31 (2015) 1193–1197.
[4] Z. Zhang, H.M. Jin, J.W. Chai, J.S. Pan, H.L. Seng, G.T.W. Goh, L.M. Wong, M.B. Sullivan, S.J. Wang, Temperature-dependent microstructural evolution of Ti_2AlN thin films deposited by reactive magnetron sputtering, Appl. Surf. Sci. 368 (2016) 88–96.

[5] M. Beckers, N. Schell, R.M.S. Martins, A. Mücklich, W. Möller, L. Hultman, Microstructure and nonbasal-plane growth of epitaxial Ti_2AlN thin films, J. Appl. Phys. 99 (2006) 034902.
[6] M. Beckers, N. Schell, R.M.S. Martins, A. Mucklich, W. Moller, L. Hultman, Nucleation and growth of Ti_2AlN thin films deposited by reactive magnetron sputtering onto MgO(111), J. Appl. Phys. 102 (2007) 074916.
[7] M. Beckers, C. Höglund, C. Baehtz, R.M.S. Martins, P.O.Å. Persson, L. Hultman, W. Möller, The influence of substrate temperature and Al mobility on the microstructural evolution of magnetron sputtered ternary Ti-Al-N thin films, J. Appl. Phys. 106 (2009) 064915.
[8] H.M. Jin, Z. Zhang, Y.G. Nie, Y.Z. Zeng, L. Shen, M.B. Sullivan, S.J. Wang, Interfacial structure of Ti_2AlN thin films on MgO(111), J. Phys. Chem. C 117 (2013) 16515–16522.
[9] T.F. Zhang, Q.M. Wang, J. Lee, P.L. Ke, R. Nowak, K.H. Kim, Nanocrystalline thin films synthesized from a Ti_2AlN compound target by high power impulse magnetron sputtering technique, Surf. Coat. Technol. 212 (2012) 199–206.
[10] Y. Yang, M. Keunecke, C. Stein, L.J. Gao, J. Gong, X. Jiang, K. Bewilogua, Chao Sun, Formation of Ti_2AlN phase after post-heat treatment of Ti-Al-N films deposited by pulsed magnetron sputtering, Surf. Coat. Technol. 206 (2012) 2661–2666.
[11] Q.M. Wang, W. Garkas, A.F. Renteria, C. Leyens, K.H. Kim, Oxidation behaviour of Ti_2AlN films composed mainly of nanolaminated MAX phase, J. Nanosci. Nanotechnol. 11 (2011) 8959–8966.
[12] Z. Zhang, H.M. Jin, J.W. Chai, L. Shen, H.L. Seng, J.S. Pan, L.M. Wong, M.B. Sullivan, S.J. Wang, Desorption of Al and phase transformation of Ti_2AlN MAX thin film upon annealing in ultra-High-Vacuum, J. Phys. Chem. C 118 (2014) 20927–20939.
[13] Y.H. Zhao, L. Xu, C.Q. Guo, W.J. Yang, G.Q. Lin, B.H. Yu, Effect of axial magnetic field on the microstructure and mechanical properties of CrN films deposited by arc ion plating, Acta Metall. Sin. 29 (2016) 546–553.
[14] P. Sathrum, B.F. Coll, Plasma and deposition enhancement by modified arc evaporation source, Surf. Coat. Technol. 50 (1992) 103–109.
[15] S.Y. Zhou, S.J. Yan, B. Han, B. Yang, B.Z. Lin, Z.D. Zhang, Z.W. Ai, V.O. Pelenovich, D.J. Fu, Influence of modulation period and modulation ratio on structure and mechanical properties of TiBN/CrN coatings deposited by multi-arc ion plating, Appl. Surf. Sci. 351 (2015) 1116–1121.
[16] L.L. Wang, R.Y. Wang, S.J. Yan, R. Zhang, B. Yang, Z.D. Zhang, Z.H. Huang, D.J. Fu, Structure and properties of Mo-containing diamond-like carbon films produced by ion source assisted cathodic arc ion-plating, Appl. Surf. Sci. 286 (2013) 109–114.
[17] J. Rosén, L. Ryves, P.O.Å. Persson, M.M.M. Bilek, Deposition of epitaxial Ti_2AlC thin films by pulsed cathodic arc, J. Appl. Phys. 101 (2007) 056101.
[18] M.C. Guenette, M.D. Tucker, M. Ionescu, M.M.M. Bilek, D.R. McKenzie, Cathodic arc co-deposition of highly oriented hexagonal Ti and Ti_2AlC MAX phase thin film, Thin Solid Films 519 (2010) 766–769.
[19] J.J. Li, Y.H. Qian, D. Niu, M.M. Zhang, Z.M. Liu, M.S. Li, Phase formation and microstructure evolution of arc ion deposited Cr_2AlC coating after heat treatment, Appl. Surf. Sci. 263 (2013) 457–464.
[20] D.J. Kong, H.Y. Guo, Friction-wear behaviors of cathodic arc ion plating AlTiN coatings at high temperatures, Tribol. Int. 88 (2015) 31–39.
[21] P.O.A. Persson, S. Kodambaka, I. Petrov, L. Hultman, Epitaxial $Ti_2AlN(0001)$ thin film deposition by dual-target reactive magnetron sputtering, Acta Mater. 55 (2007) 4401–4407.
[22] J. Xu, L. Liu, Z. Li, P. Munroe, Z.-H. Xie, Niobium addition enhancing the corrosion resistance of nanocrystalline Ti_5Si_3 coating in H_2SO_4 solution, Acta Mater. 63 (2014) 245–260.
[23] R.M. Langford, A.K. Petford-Long, Preparation of transmission electron microscopy cross-section specimens using focused ion beam milling, J. Vac. Sci. Technol. A 19 (2001) 2186.
[24] T.F. Zhang, H.-b. Myoung, D.-W. Shin, K.H. Kim, Syntheses and properties of Ti_2AlN MAX-phase films, J. Ceram. Process. Res. 13 (2012) 149–153.
[25] L.B. Kong, T.S. Zhang, J. Ma, F. Boey, Progress in synthesis of ferroelectric ceramic materials via high-energy mechanochemical technique, Prog. Mater. Sci. 53 (2008) 207–322.
[26] X. Kuang, G. Carotenuto, L. Nicolais, A review of ceramic sintering and suggestions on reducing sintering temperatures, Adv. Perform. Mater. 4 (1997) 257–274.
[27] V. Presser, M. Naguib, L. Chaput, A. Togo, G. Hug, M.W. Barsoum, First-order Raman scattering of the MAX phases: Ti_2AlN, $Ti_2AlC_{0.5}N_{0.5}$, Ti_2AlC, $(Ti_{0.5}V_{0.5})_2AlC$, V_2AlC, Ti_3AlC_2, and Ti_3GeC_2, J. Raman Spectrosc. 43 (2012) 168–172.
[28] M.N. Solovan, V.V. Brusa, P.D. Maryanchuk, T.T. Kovalyuk, J. Rappich, M. Gluba, Kinetic properties of TiN thin films prepared by reactive magnetron sputtering, Phys. Solid State 55 (2013) 2234–2238.
[29] T. Cabioc'h, P. Eklund, V. Mauchamp, M. Jaouen, Structural investigation of substoichiometry and solid solution effects in $Ti_2Al(C_x,N_{1-x})_y$ compounds, J. Eur. Ceram. Soc. 32 (2012) 1803–1811.
[30] B. Cui, R. Sa, D.D. Jayaseelan, F. Inam, M.J. Reece, W.E. Lee, Microstructural evolution during high-temperature oxidation of spark plasma sintered Ti_2AlN ceramics, Acta Mater. 60 (2012) 1079–1092.
[31] M. Pohler, R. Franz, J. Ramm, P. Polcik, C. Mitterer, Cathodic arc deposition of $(Al,Cr)_2O_3$: macroparticles and cathode surface modifications, Surf. Coat. Technol. 206 (2011) 1454–1460.
[32] S.J. Pennycook, B. Rafferty, P.D. Nellist, Z-contrast imaging in an aberration-corrected scanning transmission electron microscope, Microsc. Microanal. 6 (2000) 343–352.
[33] Q. Huang, H. Han, R.D. Liu, G.H. Lei, L. Yan, J. Zhou, Q. Huang, Saturation of ion irradiation effects in MAX phase Cr_2AlC, Acta Mater. 110 (2016) 1–7.
[34] M. Bugnet, T. Cabioc'h, V. Mauchamp, Ph. Guerin, M. Marteau, M. Jaouen, Stability of the nitrogen-deficient Ti_2AlN_x MAX phase in Ar^{2+}-irradiated (Ti, Al)N/Ti_2AlN_x multilayers, J. Mater. Sci. 45 (2010) 5547–5552.
[35] H.C. Barshilia, K.S. Rajam, Raman spectroscopy studies on the thermal stability of TiN, CrN TiAlN coatings and nanolayered TiN/CrN, TiAlN/CrN multilayer coatings, J. Mater. Res. 19 (2004) 3196–3205.
[36] V. Dolique, M. Jaouen, T. Cabioc'h, F. Pailloux, P. Guérin, V. Pélosin, Formation of (Ti,Al)N/Ti_2AlN multilayers after annealing of TiN/TiAl(N) multilayers deposited by ion beam sputtering, J. Appl. Phys. 103 (2008) 083527.
[37] T. Cabioch, M. Alkazaz, M.F. Beaufort, J. Nicolai, D. Eyidi, P. Eklund, Ti_2AlN thin films synthesized by annealing of (Ti + Al)/AlN multilayers, Mater. Res. Bull. 80 (2016) 58–63.
[38] R. Grieseler, T. Kups, M. Wilke, M. Hopfeld, P. Schaaf, Formation of Ti_2AlN nanolaminate films by multilayer-deposition and subsequent rapid thermal annealing, Mater. Lett. 82 (2012) 74–77.
[39] M. Beckers, N. Schell, R.M.S. Martins, A. Mücklich, W. Möller, Phase stability of epitaxially grown Ti_2AlN thin films, Appl. Phys. Lett. 89 (2006) 074101.